

ON THE ORTHORHOMBIC DISTORTION OF $\text{CaMnO}_{3-\delta}$

© Paszkowicz W., Piętosza J, 2007

CaMnO_3 , is a parent compound for numerous multicomponent manganites. Its crystallographic data are of importance in studies of materials having CaMnO_3 as a component. Its orthorhombic structure can be treated as weakly distorted cubic one. The magnitude of orthorhombic distortion may be influenced by the possible excess from stoichiometry as well as by technology-dependent defect structure. In this paper, the distortion is discussed on the basis of literature data coming from various laboratories. It is concluded that these data (both, stoichiometric and off-stoichiometric) show a large scatter of distortion magnitude. However, those of highest accuracy in lattice parameter values, reported in the last decade, are consistent, indicating that they can be treated as most reliable ones. Trends in the influence of oxygen off-stoichiometry on the distortion and the need of further experimental studies are pointed out. The results of the present analysis can be useful in structural studies of CaMnO_3 -based solid solutions.

1. Introduction

Perovskite oxides (ABO_3 with A = divalent alkaline-earth metal ion or trivalent rare earth metal ion, B = a transition metal ion), exhibit interesting physical properties. These properties are connected with the occurrence, in specific materials of this kind, of the phenomena such as Jahn-Teller distortion, different valence states of the transition metal ions, charge ordering, ionic conductivity, superconductivity¹, ferromagnetism, ferroelectricity, piezoelectricity, and the colossal magnetoresistance effect. The structural framework of cubic perovskite permits for distortions, which lower the symmetry of the system, as, for instance, for CaMnO_3 . This compound is a G-type noncollinear antiferromagnetic (AFM) insulator² with additional weak ferromagnetic component in its ground state [1]. CaMnO_3 , one of numerous compounds existing in the Ca-Mn-O system, is used as a parent compound for various manganite systems such as $\text{La}_{1-x}\text{Ca}_x\text{MnO}_3$ and $\text{Sr}_{1-x}\text{Ca}_x\text{MnO}_3$.

At ambient conditions, CaMnO_3 exhibits a perovskite-type structure ($Z=4$, space group $Pnma$, [2]), with a GdFeO_3 -type orthorhombic unit cell. Initially, due to undetectability of minor orthorhombic distortion, a primitive cubic unit cell with $a = 7.46 \text{ \AA}$ [3,4]) has been ascribed to this compound. The basic cubic perovskite cell has been also used in earlier theoretical considerations in order to simplify the time-consuming calculations [5].

The aim of this work is the analysis of CaMnO_3 orthorhombic distortion on the basis of existing literature data.

2. Magnitude of orthorhombic distortion

A survey of available unit-cell-size data for orthorhombic CaMnO_3 reveals the relatively large discrepancies between lattice parameters reported by various groups for stoichiometric samples, at room temperature and ambient pressure. The differences largely exceed the (frequently small) error bounds (see Table 1). Lattice parameters of CaMnO_3 can be presented in a dimensionless form, as in the graph (Fig. 1), with b/a and c/a values at the axes. This pair of axial ratios describes the magnitude of orthorhombic distortion. The data displayed in Fig. 1 involve the axial ratios for both, stoichiometric ($\delta=0$) and non-stoichiometric ($\delta>0$) $\text{CaMnO}_{3-\delta}$. The distortion of CaMnO_3 is considerably smaller than that for many orthorhombic perovskites. Consequently, to determine the lattice parameters, the experimental and computational requirements are specifically high. In particular, the instrument resolution must be high and the counting statistics of the collected data must be very good.

¹ $(\text{Ba},\text{X})\text{BiO}_3$ superconductors exhibit T_c up to about 30 K

² For the G-type configuration, each Mn^{4+} ion has six Mn^{4+} neighbours with spins being antiparallel to the central ion

The way of presentation used in Fig. 1 i) tends to eliminate the systematic errors of lattice parameters; such errors in diffraction measurements, due to inaccuracies connected with sample position, X-ray absorption, uncertainties in angular scale and X-ray wavelength, affect mainly the absolute values, ii) informs about the axial ratios, *i.e.* about the orthorhombic distortion [the zero distortion is represented by the point ($\sqrt{2}$, 1)].

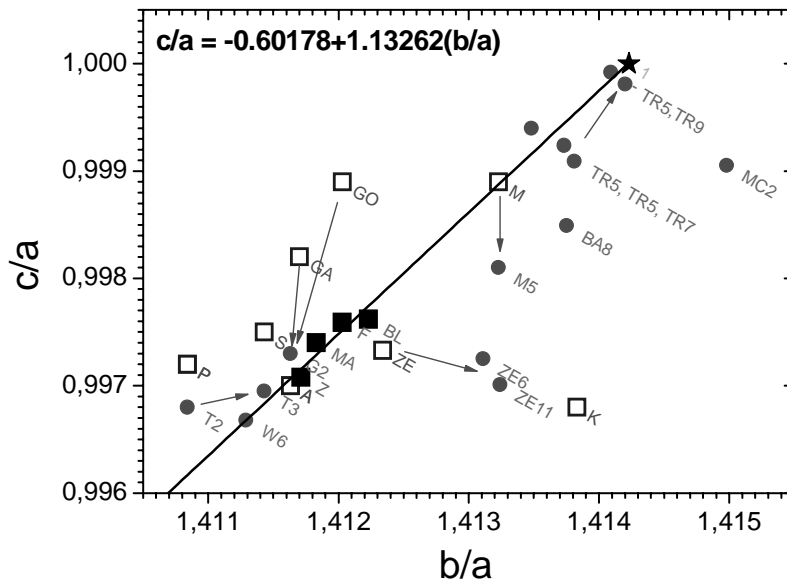


Figure 1. Orthorhombic distortion for $\text{CaMnO}_{3-\delta}$, shown through correlation between the b/a and c/a axial ratios. The axial ratio values were extracted from room-temperature data of samples reported in the cited papers. Four points (represented by full squares) corresponding to the highest accuracy reported in four distinct papers for stoichiometric compound are located at a straight line passing through the point ($\sqrt{2}$, 1) representing the ideal (undistorted) structure. The selected four points are those of recent Rietveld refined data with the standard deviations 0.0004 \AA or better for all three lattice parameters. Positions of 5 points representing lower precision (open squares) and 14 those referring to samples with oxygen vacancies (full circles) are discussed in the text. Errors of the axial ratios are generally smaller than the symbol size

Arrows indicate the direction of changes when increasing the amount of oxygen vacancies; the percentage of vacancies is denoted by a one- or two-digit numbers representing the δ value

Symbols (from left to right in the graph):: P [2], T2($\delta=0.02$) [6], T3($\delta=0.03$) [7], W6 [8], S [9], A [10], G2($\delta=0.02$), GA (sample prepared in air), GO (sample prepared in oxygen) [11], Z [12], MA [13], F [14], BL [15], ZE, ZE6 ($\delta=0.06$), Ze11 ($\delta=0.11$) [16], M, M5 ($\delta=0.05$) [17], TR5, TR7, TR9 ($\delta=0.05$ three samples, 0.07, 0.09) [18], BA8($\delta=0.08$) [19], K [20], MC2 ($\delta=0.02$) [1], starred: undistorted cell. The solid line represents the least squares fit for four data of the smallest error values and the point for undistorted perovskite. Arrows represent the direction of shifts occurring when δ increases, as reported by various authors.

The distortion, represented by a point at the graph, is expected to depend on the composition and defect structure. Assuming that there are no calculation errors, the positions of points at the graph should depend only on composition (off-stoichiometry, impurities) and sample preparation method. The effect of thermal expansion on axial ratios was derived from the data of Ref. [12]. Its magnitude in the room temperature region appears to be less than the size of the symbols plotted in Fig. 1. Therefore, the temperature cannot be responsible for the differences between data displayed in Fig. 1.

It is worth noting that the data shown in the graph exhibit some interesting features although they come from quite different authors and samples synthesised using various techniques.

Data for stoichiometric samples

The relative b/a and c/a variability ranges for stoichiometric ($x=0$) samples are relatively large, 0.2% and 0.3%, respectively. When distinguishing the points representing the recent stoichiometric data of highest reported accuracy, one finds that they are grouped around the point (1.412, 0.9974). Four datasets of highest accuracy (those quoted in Part 1 of the Table 1) are contained within the narrow ranges $1.4117 < b/a < 1.4122$ and $0.9971 < c/a < 0.9976$. Within this group, the data of Ref. [12] are of particular value, because i) of the experimental technique involving synchrotron X-ray beam providing the best resolution and excellent counting statistics (both are important in the present case of strong peak overlap) and ii) the reported accuracy is the highest among all data available for the present authors. A straight line with fitted coefficients (the performed fittings included the four points and the point representing the undistorted structure) defined by the formula

$$(c/a) = -0.60178 + 1.13262 \times (b/a) \quad (1)$$

shown in Fig. 1 can serve as a basis for discussion of the distortion magnitude. Three more stoichiometric data of lower accuracy [9, 10, 16] are in the close vicinity of the four points. Remaining five data with lower accuracy reported are apparently more dispersed than the above-mentioned ones. A tendency (with only several exceptions) is observed that the stoichiometric samples are located at or above the reference line, whereas the oxygen-deficient samples are at or below this line.

Table 1. Lattice parameters of $\text{CaMnO}_{3-\delta}$ (space group $Pnma$)

Starred are those pseudocubic cells. LXR - laboratory X-ray diffraction. SXRD - synchrotron X-ray diffraction. The cited papers refer to study of polycrystalline except the case denoted "mono". ND refers to neutron diffraction. Abbreviation "Riet" is added for cases where the results are obtained through Rietveld refinement of powder diffraction data. LSQ - least squares refinement, RNR - refinement method not reported

Part 1 - data with the highest precision reported. Part 2 - data with lower or unreported precision. Part 3 - off-stoichiometric samples. RT refers to room temperature, NQ - temperature not quoted. Some references are completed by numbers of records in the ICDD and ICSD databases.

x	a [Å] .008	b [Å] .005	c [Å] 0.007	b/a	c/b	c/a	V	V_{fu}	T (K)	method	Reference	Year
Part 1												
0	5.28287(5)	7.45790(7)	5.26746(5)	1.41171	0.70629	0.99708	207.53	51.882	298	SXRD(Riet)	[12]	2006
(*)	5.2754(2)	7.4478(3)	5.2617(2)	1.41180	0.70648	0.9974	206.73	51.682		ND(Riet)	[13]; ICSD 94058	2001...
0	5.2770(2)	7.4510(4)	5.2643(2)	1.41198	0.70652	0.99759	206.99	51.747		LXRD(Riet)	[14]; ICSD86645	1998
0	5.2813(1)	7.4582(1)	5.2687(1)	1.41219	0.70643	0.99762	207.53	51.882	RT	LXRD(Riet)	[15]; ICSD92083	2000
Part 2												
0	5.279(1)	7.448(1)	5.264(1)	1.41087	0.7068	0.9972	206.97	51.742	RT	LXRD (monocrystal)	[2]; ICSD35218	1982
0	5.268	7.435	5.255	1.41135	0.7068	0.9975	205.8	51.45	NQ	LXRD (Riet)	[9]	2005
0	5.281	7.455	5.265	1.41166	0.7062	0.9970	207.28	51.820	NQ	LXRD(RNR)	[10]	2006
0	5.2827(5)	7.4576(8)	5.2735(8)	1.41170	0.70713	0.9982	207.76	51.239	NQ	LXRD(Riet)	[11] sample prep. in air	2005
0	5.2812(8)	7.457(1)	5.2753(8)	1.41198	0.7074	0.9989	207.75	51.937	NQ	LXRD(Riet)	[11]; ICSD153238; sample prep. in oxygen	2005
0	5.2782(2)	7.4546(1)	5.2641(3)	1.41234	0.70615	0.99733	207.13(2)	51.782	NQ	LXRD(LSQ)	[16]	1999
0	5.279(1)	7.460(2)	5.273(1)	1.41315	0.7068	0.9989	207.66	51.915	NQ	LXRD (Riet)	[17]; ICSD93036	2001
0	5.276	7.459	5.259	1.41376	0.7051	0.9968	206.96	51.740	RT	LXRD (Riet)	[20]	2006
0	5.277(2)	7.467(5)	5.274(3)	1.41501	0.7063	0.9994	207.81	51.952		LXRD	[21]	2004
Part 3												
0.02	5.282	7.452	5.265	1.41083	0.7065	0.9968	207.24	51.810	RT	LXRD (Riet)	[6]; ICDD 46-1266	1989
0.02	5.2859(1)	7.4619(2)	5.2715(1)	1.41166	0.7065	0.9973	207.92	51.980	NQ	LXRD(Riet)	[11]; ICSD153239 ceramic sample	2005
0.02	5.275(2)	7.464(2)	5.270(2)	1.41498	0.70606	0.99905	207.49	51.873	NQ	LXRD (LSQ)	[1]	1967
0.03	5.2819 (1)	7.4547(2)	5.2658 (1)	1.41137	0.7064	0.99695	207.34	51.835	RT	LXRD(Riet)	[1]; ICDD 501746, ICSD50997	1996
0.05	5.281(5)	7.463(1)	5.271(3)	1.41318	0.7063	0.9981	207.74	51.935	NQ	LXRD (Riet)	[17]; ICSD93035	2001
0.05	5.2747(5)	7.4574(7)	5.2699(5)	1.41381	0.70667	0.99909	207.29	51.824	NQ	LXRD (RNR)	[18]	2004
0.05	5.2750(8)	7.4561(9)	5.2719(8)	1.41348	0.70706	0.99941	207.35	51.837	NQ	LXRD (RNR)	[18]	2004
0.05	5.2737(6)	7.4574(9)	5.2733(6)	1.41407	0.70712	0.99992	207.39	51.847	NQ	LXRD (RNR)	[18]	2004
0.06	5.2792(2)	7.4601(1)	5.2647(3)	1.41311	0.70571	0.99725	207.34(2)	51.835	NQ	LXRD (LSQ)	[16]	1999
0.06	5.2729(6)	7.4416(6)	5.2554(6)	1.41129	0.70622	0.99668	206.22	51.554	RT	ND(Riet)	[8]	2001
0.07	5.274(1)	7.456(1)	5.270(1)	1.41373	0.70681	0.99924	207.23	51.808	NQ	LXRD (RNR)	[18]	2004
(0.08)	5.281(1)	7.466(1)	5.273(1)	1.41375	0.70627	0.99849	207.90	51.976	RT		[19]	2005
0.09	5.2728(4)	7.4568(6)	5.2718(4)	1.41420	0.70698	0.99981	207.28	51.819	NQ	LXRD (RNR)	[18]	2004
0.11	5.2802(1)	7.4622(2)	5.2644(1)	1.41324	0.70548	0.99701	207.42(1)	51.855	NQ	LXRD (LSQ)	[16]	1999

(*) excess oxygen suggested by the refinements

Data for off-stoichiometric samples

In the figure, arrows indicate the results of several laboratories studying the effect of reducing the δ value on lattice parameters. Each arrow indicates the direction of rising δ , while the value of δ is included in the given symbol label (see the figure legend).

Table 2. Magnitude of c/b variation with increasing δ value.

Points in Fig. 1	$\Delta(c/b)$	$\Delta(c/b)/\Delta\delta$ [%]
ZE \rightarrow ZE6	0.70615 \rightarrow 0.70571	0.007
M \rightarrow M5	0.70684 \rightarrow 0.70638	0.011
T2 \rightarrow T3	0.70652 \rightarrow 0.70637	0.015
GO/GA \rightarrow G2	0.70713 \rightarrow 0.70646 0.70742 \rightarrow 0.70646	0.033, 0.048

Neglecting the data of Ref. [18] (they exhibit extremely weak distortion for all samples) one can conclude that the increase of δ leads to unchanged or reduced c/a whereas the b/a remains constant or increases. Consequently, the c/b ratio tends to decrease, with increasing δ , for all samples from four laboratories [6, 7, 11, 16, 17], as quoted in Table 2. It is worth noting that the changing rate (expressed by $\Delta(c/b)/\Delta\delta$) is about 0.01, i.e. similar for data for three among four datasets, although they come from quite different authors and different samples.

The above-suggested tendency in c/b variation with δ is on data for samples which may differ in composition and defect structure. In order to draw clear conclusions concerning the distortion variation of $\text{CaMnO}_{3-\delta}$ with varying δ value, detailed diffraction studies for carefully prepared samples differing in δ value are needed.

There may exist other factors influencing the lattice parameters and their ratios. In particular the Ca:Mn ratio may exhibit some deviation from unity for certain samples, and the defect structure (e.g., the presence of vacancies) may differ among the nominally identical samples of various laboratories. Studies of the effect of such other factors are still missing in literature.

Understanding of the orthorhombic lattice parameter values and distortions of $\text{CaMnO}_{3-\delta}$ is important for analysis of physical properties of $\text{CaMnO}_{3-\delta}$ containing solid solutions, in particular their magnetic properties. Moreover, the knowledge of the considered data may be useful in analysis of presence and exact chemical composition of CaMnO_3 in decomposition product of Mn-containing dolomite-like rocks and some industrial deposits (presence of such materials has been reported in Refs [22] and [23], respectively).

3. Conclusions

Large discrepancies exist among lattice parameters reported for stoichiometric CaMnO_3 and among the magnitudes of distortion at ambient conditions. In this paper both, the lattice parameters and the magnitude of orthorhombic distortion are discussed for CaMnO_3 compound on the basis of literature data coming from various laboratories. It is concluded that these data show a large scatter of distortion values, but those of highest reported accuracy in lattice parameter values, reported in the last decade, are consistent indicating that just they can be treated as most reliable ones. The most accurate data are grouped around the point $(b/a, c/a) = (1.412, 0.9974)$. A reference line roughly separates the domains where the reported samples are stoichiometric ($\delta=0$) and off-stoichiometric ($\delta>0$). Different distortion dependence on oxygen off-stoichiometry, observed in different literature sources, is discussed. The results of the present analysis can be useful in structural studies of CaMnO_3 -based solid solutions and related materials.

1. J.B. MacChesney, H.J. Williams, J.F. Potter, R.C. Sherwood, *Magnetic Study of the Manganate Phases: CaMnO_3 , $\text{Ca}_4\text{Mn}_3\text{O}_{10}$, $\text{Ca}_3\text{Mn}_2\text{O}_7$, Ca_2MnO_4* , *Phys. Rev.* 164, 779 (1967). 2. R. Poeppelmeier, M.E. Leonowicz, J.C. Scanlon, J.M. Longo, W.B. Yelon, *Structure determination of CaMnO_3 and $\text{CaMnO}_{2.5}$ by X-ray and neutron methods*, *J. Solid State Chem.* 45, 71 (1982). 3. ICDD 3830 (*International Centre for Diffraction Data 2001*). 4. E. O. Wollan and W. C. Koehler, *Neutron Diffraction*

Study of the Magnetic Properties of the Series of Perovskite-Type Compounds [(1-x)La,xCa]MnO₃, *Phys. Rev.* 100, 545 – 563 (1955). 5. F. Freyria Fava, Ph. D'Arco, R Orlando, R. Dovesi, A quantum mechanical investigation of the electronic and magnetic properties of CaMnO₃ perovskite, *J. Phys.: Condens. Matter* 9 (1997) 489–498. 6. Taguchi H., Nagao M., Sato T., Shimada M., High-temperature phase transition of CaMnO_{3-δ}, *J. Solid State Chem.* 78 (1989) 312. 7. H. Taguchi, Relationship between Crystal Structure and Electrical Properties of the Ca-Rich Region in (La_{1-x}Ca_x)MnO_{2.97}, *J. Solid State Chem.* 124, 360–365 (1996). 8. C.R. Wiebe, J. E. Greedan, J. S. Gardner, Z. Zeng and M. Greenblatt, Charge and magnetic ordering in the electron-doped magnetoresistive materials CaMnO_{3-δ}, δ=0.06, 0.11, *Phys. Rev. B* 64 (2001) 064421. 9. B.V. Slobodin, E.V. Vladimirova, S.L. Petukhov, L.L. Surat, I.A. Leonidov, Synthesis and Structure of (Ca,Sr)-Substituted Lanthanum Manganite, *Inorganic Materials*, Vol. 41, No. 8, 2005, pp. 869–875. Translated from *Neorganicheskie Materialy* 41,2005, 990–997. 10. R. Ang, Y.P. Sun, Y.Q. Ma, X.B. Zhu, W.H. Song, Diamagnetism and relative Young's modulus in the perovskite manganites CaMn_{1-x}V_xO₃ (0 ≤ x ≤ 0.08), *Solid State Communications* 140 (2006) 416–421. 11. I. Gil de Muro; M. Insausti, L. Lezama; T. Rojo, Morphological and magnetic study of CaMnO_{3-x} oxides obtained from different routes, *Journal of Solid State Chemistry* 178 (2005) 928-936. 12. Q. Zhou, B.J. Kennedy, Thermal expansion and structure of orthorhombic CaMnO₃, *Journal of Physics and Chemistry of Solids* 67 (2006) 1595–1598. 13. A. Machida, Y. Moritomo, K. Ohoyama, A. Nakamura, Neutron investigation of Tb_{1-x}Ca_xMnO₃ (x ≥ 0.5), *J. Phys. Soc. Jpn* 70 (2001) 3739–3746. 14. I.D. Fawcett, J.E. Sunstrom, IV, M. Greenblatt, M Croft, K.V.Ramanujachary, Structure, magnetism, and properties of Ruddlesden-Popper calcium manganates prepared from citrate gels, *Chemistry of Materials* (1998), 10, 3643-3651, (ALSO P. Tomaszewski, *Golden Book of Phase Transitions*, Wroclaw (2002), 1, 1–123). 15. J. Blasco, C.Ritter, J.Garcia, J.M., de Teresa, J. Perez-Cacho, M.R. Ibarra, Structural and magnetic study of Tb_{1-x}Ca_xMnO₃ perovskites, *Physical Review B* (2000), 62(9), 5609–5618. 16. Z. Zeng, M. Greenblatt, M. Croft, Large magnetoresistance in antiferromagnetic CaMnO_{3-δ}, *Phys. Rev. B* 59, 13 (1999) 878. 17. M.E. Melo Jorge, A. Correia dos Santos, M.R.Nunes, Effects of synthesis method on stoichiometry, structure and electrical conductivity of CaMnO_{3-δ}, *Int. J. Inorg. Mater.* (2001), 3, 915–921. 18. J. Töpfer, U. Pippardt, I. Voigt, R. Kriegel, Structure, nonstoichiometry and magnetic properties of the perovskites Sr_{1-x}Ca_xMnO_{3-δ}, *Solid State Sciences* 6 (2004) 647–654. 19. E. Bakken, T. Norby, S. Stølen, Nonstoichiometry and reductive decomposition of CaMnO_{3-δ}, *Solid State Ionics* 176 (2005) 217–223. 20. M. Kar, S.M. Borah, S. Ravi, Study of electrical transport and magnetic properties, in CaMn_{1-x}Cu_xO₃, *Materials Science and Engineering B* 129 (2006) 54–58. 21. L. Rørmark, K. Wiik, S. Stølen, T. Grande, Oxygen stoichiometry and structural properties of La_{1-x}A_xMnO_{3-d} (A= Ca or Sr and 0<x<1), *J. Mater. Chem.*, 2002, 12, 1058–1067. 22. A.R. Fazeli, J. A. K. Tareen, Thermal decomposition of rhombohedral double carbonates of dolomite type, *Journal of Thermal Analysis* 37 (1991) 2605–2611. 23. H. Bilinski, Ž. Kwokal, M. Branica, Formation of some manganese minerals from ferromanganese factory waste disposed in the Krka river estuary, *Wat. Res.* 30 (1996) 495–500.